4-10-2017

Statistical modeling of the fuel flow rate of GA piston engine aircraft using flight operational data

Chenyu "Victor" Huang

Yixi Xu

Mary E. Johnson

Statistical modeling of the fuel flow rate of GA piston engine aircraft using flight operational data

Chenyu Huang [⇑], Yixi Xu [1], Mary E. Johnson [2]

Purdue University, West Lafayette, IN 47906, USA

⇑ Corresponding author at: School of Aviation and Transportation Technology, Purdue University, 1401 Aviation Drive, West Lafayette, IN 47906, USA. *E-mail address:* huang659@purdue.edu (C. Huang).

[1] Department of Statistics, Purdue University, 250 N. University Street, West Lafayette, IN 47907, USA.

[2] School of Aviation and Transportation Technology, Purdue University, 1401 Aviation Drive, West Lafayette, IN 47906, USA.

http://dx.doi.org/10.1016/j.trd.2017.03.023

Keywords: General aviation, Fuel flow rate, Statistical modeling, Flight data

ABSTRACT

The United States has the largest and most diverse general aviation (GA) community in the world, with more than 220,000 aircraft, flying almost 23 million hours annually. Accurate and economic estimating the exhaust emissions of general aviation will effectively support the practice of mitigating the environmental impacts from general aviation. Fuel flow rate in each phase of the Landing and Takeoff Cycle is one of the necessary factors recommended by the International Civil Aviation Organization to be used to estimate the exhaust emissions. This paper explores statistical models of predicting the fuel flow rate of piston- engine aircraft using general aviation flight operational data, including the aircraft altitude, the ground speed, and the vertical speed. A machine learning technique is applied to adapt the variability of flight operational data due to flexible operations of general aviation and random errors in flight data. The Classification and Regression Trees (CART) and the Smoothing Spline ANOVA (SS-ANOVA) are adopted as the modeling approaches. The modeling results are compared and interpreted from the

standpoint of general aviation phases of flight in the Landing and Takeoff Cycle. Both models demonstrate good accuracy in predicting the fuel flow rate. The CART model provides intuitive outputs by the phases of flight, and is more robust to flight data outliers. The SS-ANOVA model is relatively more accurate in predicting the fuel flow rate, and is better at explaining the interaction between variables. A robust fuel flow rate prediction model of predicting the fuel flow rate of piston- engine aircraft is believed to be practical and economic for GA exhaust emissions estimation.

Introduction

With the rapid development of aviation technology during the past decades, both global and regional economies have benefited from the fast, efficient, and worldwide air transportation. While commercial air transport services carry large portion of passengers and freight, general aviation (GA) is sharing a considerable part of the air transportation market with an estimated annual shipment billings of 24,120 million U.S. dollars (General Aviation Manufacturers Association, 2016). While people are enjoying the convenience of modern air transport, aviation also generates remarkable environmental impacts. To mitigate the impact on the environment from aviation activities, the Committee on Aviation Environment Protection (CAEP) was established in 1983 as a technical committee of the International Civil Aviation Organization (ICAO) to assist the council in formulating policies and adopting Standards and Recommended Practices (SARPs) related to aircraft noise and emissions, and more generally to aviation environmental impact (International Civil Aviation Organization, 2016a,b). Following the ICAO, government agencies and other organizations, such as the International Air Transport Association (IATA), Federal Aviation Administration (FAA), EUROCONTROL, Swiss Federal Office of Civil Aviation (FOCA), National Aeronautics and Space Administration (NASA), and the U.S. Environmental Protection Agency (EPA) also conducted a series of practices to alleviate the environmental impact from different perspectives (International Air Transport Association, 2013; Federal Aviation Administration, 2005; European Union, 2008; Swiss Federal Office of Civil Aviation,

2007; U.S. Environmental Protection Agency, 1985).

With the goals of reducing the impact of aviation emissions on local air quality, and reducing the impact of aviation greenhouse gas emission on the global climate, IATA proposed the four-pillar strategy to neutralize the carbon emission from aviation, which includes the development of advanced technology, adopting more efficient aircraft operations, improving present infrastructure, and economic measures (International Air Transport Association, 2016). ICAO also proposed the standards for emission certification of aircraft turbine engines which currently cover carbon monoxide (CO), unburned hydrocarbons (HC), oxides of nitrogen (NO_x) and smoke (SN) (International Civil Aviation Organization, 2008, 2011). In order to measure the effectiveness of approaches to reducing aviation emissions, various tools have been developed to measure the volume of different types of aviation emissions. Early in mid-1980s, the Emissions and Dispersion Modeling System (EDMS) was developed. EDMS was used by the US EPA to evaluate aviation emissions, which was replaced by a more sophisticated tool – the Aviation Environment Design Tool, Version 2c (AEDT, V.2c) as of December 2016 (U.S. Federal Aviation Administration, 2017). The Advanced Emissions Model (AEM), the Airport Local Air Quality Studies (Open-ALAQS), the IMPACT are examples of other modeling tools for aircraft noise and emissions assessments (EUROCONTROL, 2016).

The ICAO recommended concept of Landing and Takeoff Cycle (LTO) is widely used in environmental modeling tools to measure and estimate aviation emissions by phases of flight. The LTO cycle consists of four phases of flight – taxi, takeoff, climb-out, and approach, under the mixing height altitude, which is generally 3000 ft (915 m) above the ground level (AGL) (International Civil Aviation Organization, 2008). Based on the engine mode in each phase of flight, the exhaust emissions are calculated with the function (1) (International Civil Aviation Organization, 2008).

$$\textit{Total Emissions of pollutant } j = \sum\left(EI_{ij} * FFR_i * DUR_i * LTO_i\right) \qquad (1)$$

where $EI_{i,j}$ = aircraft engine emission index for a specific pollutant of *j* in the phase of flight of *i* (kg-exhaust chemical/kg-fuel burned), FFR_i = the average fuel flow rate in the phase of flight of *i* (kg-fuel/s), *i* = phase of flight (taxi/idle, takeoff, climb-out, approach), DUR_i = the duration of the phase of flight of *i* (s), LTO_i = the number of the phase of

flight of *i* per aircraft type during a time period, and R = the sum of each phase of flight in LTO cycle.

As an important part of aviation sector, the general aviation community has greatly supported and contributed to the fast growth of entire aviation industry. Today, there are more than 362,000 general aviation aircraft worldwide, of which 204,000 are registered in the United States flying almost 23 million hours annually across more than 5000 U.S. airports (General Aviation Manufacturers Association, 2016). General aviation activities have an environmental impact. Unlike the Commercial Air Transport, which is generally consists of turbine-engine aircraft, more than 82% of General Aviation aircraft are piston- engine aircraft (U.S. Federal Aviation Administration, 2014). Because of the diverse aircraft types in the GA fleet, the different flight performance of piston-engine aircraft from turbine-engine aircraft, and the operational flexibility, the aviation emissions assessment methods and procedures recommended by ICAO are not likely able to directly output accurate evaluation on GA emissions. In addition, GA operators and GA airports usually have very limited resources to be spent on emission assessment compared to commercial airlines and commercial service airports. Therefore, developing a feasible low-cost method to accurately estimate the exhaust emissions is believed to be practical for sustainable development of general aviation.

Among different aviation emissions assessment approaches, fuel flow rate is crucial for estimating emission volume. Currently, fuel flow rate could be obtained in many ways, such as the real-time fuel flow rate recorded by flight data recorder (FDR), and the aircraft engine specifications provided by original equipment manufacturers. However, obtaining fuel flow rate in those methods is typically time-consuming, inconvenient, inaccurate, and not quite practical in estimating GA exhaust emissions. An inexpensive and convenient way to acquire the fuel flow rate of GA piston-engine aircraft is more likely to meet the characteristics and demand of general aviation. Modeling the fuel flow rate as a function of other aircraft parameters is believed to be a good approach because there might be convenient and inexpensive ways to obtain other aircraft parameters as the explanatory variables. In 2014, Baklacioglu developed a fuel flow rate model for the climbing phase of flight using genetic algorithm method (Baklacioglu, 2016a,b). Later in 2016, Baklacioglu proposed a genetic algorithm-

optimized neural network topology to predict the fuel flow rate (Baklacioglu, 2016a,b). In the same year, Chati and Balakrishnan modeled the fuel flow rate in the airborne phases of flight with turbofan aircraft operational data from Flight Data Recorders (FDR) (Chati and Balakrishnan, 2016).

Different from commercial flights which are operating with clear phases of flight and prescribed flight procedures, most GA operations are not based on regular schedules, and many of GA aircraft are flying in Visual Flight Rules (VFR) (Huang and Johnson, 2016). What's more, aircraft piston engine demonstrates remarkable different performance from aircraft turbine engine. The previous studies are based on the flight data of commercial turbofan-engine aircraft, which may not be applicable for GA piston-engine aircraft. Therefore, predicting the fuel flow rate of fix-wing reciprocating-engine GA air- craft with those models may result in errors. This paper presents research on modeling the fuel flow rate of GA piston-engine aircraft which could be used in estimating the gaseous and particulate matters emissions of aircraft with the same type of piston engine. The methods are expected to be references for modeling the fuel flow rate of other types of aircraft piston engines.

Methodology

This section describes the collection of data used in the modeling method, and explains the variable selection and modeling methods. The modeling methods explored in this paper are the Classification and Regression Trees (CART) and the Smoothing Spline ANOVA (SS-ANOVA) models.

Data collection

General aviation piston-engine aircraft operational data were used in statistical modeling. Flight data were collected from the Cirrus SR-20 aircraft, all of which are equipped with Garmin G1000 system. G1000 system records 66 types of aircraft operational parameters every one second on average, such as 4-dimensional aircraft location, air speed, ground speed, vertical speed, and engine revolution per minute. In order to reflect the flexibility of GA operations, the flight missions were selected that include cross-country flights and local traffic pattern training flights. A total 22 flight

missions were selected and had flight durations from 77 min to 198 min. Each parameter has 176,370 observations in the dataset. All aircraft in this sample are based at Purdue University Airport, West Lafayette, Indiana.

Variables selection

The onboard flight data recorder (FDR) of Garmin G1000 provides many aircraft operational records which could be used to explore the model of estimating the fuel flow rate of GA piston-engine aircraft in all phases of flight. However, there are many factors that could affect the fuel flow rate of piston-engine aircraft; therefore, there is no standard to select explanatory variables to predict the fuel flow rate. Based on the physics of aircraft power plant operations, the fuel flow rate depends on the engine parameters, true airspeed, aircraft mass, the ambient atmospheric density, wing reference area, extra thrust for ascending, etc. (Collins, 1982). To simplify, we could assume that the ambient atmospheric density is primarily related to the altitude, and the ascent could be explained by positive vertical speed. Additionally, aircraft in this study are used for flight training that have no significant change in terms of the aircraft mass; therefore, the aircraft mass could be assumed as a constant value. Based on above simplification and assumptions, the aircraft ground speed, the altitude, and the vertical speed are initially selected as the predictors to explain the fuel flow rate in modeling. One of the crucial benefits of selecting the above explanatory variables is that there are many sources to obtain those parameters. Especially, with mandatory installation of the Automatic Dependent Surveillance – Broadcast Out (ADS-B Out) on all aircraft operating in assigned airspace by January 1, 2020, ADS-B technology is believed to be a feasible and available future data source for the model of the fuel flow rate estimation because of its capability of feeding those three explanatory variables (Part 91, 41 C.F.R. § 91.227; Part 91, 41 C.F.R.§ 91.225). The variable selection of this model is believed to satisfy the requirement of ‘‘low cost” of GA operations.

Modeling methods

Plot of selected parameters from the set of G1000 data from 22 flights are shown to better understand the nature of GA flight. Because of the brakes, temporary stops,

and the acceleration when aircraft is taxiing on the surface, aircraft engine output is changing frequently and rapidly (Khadilkar and Balakrishnan, 2012), shown as Fig. 1. Also, GA operations are relatively flexible in terms of altitude and speed, shown as Fig. 2. Generic regression methods may not be suitable for building a general model to include all phases of flight. Therefore, a machine learning technique is explored as a potential approach for future study scenario.

With the objective of discovering the relationship between the response variable and the three explanatory variables to predict the fuel flow rate from other flight data, supervised data mining algorithms are explored as possible candidates for modeling. Although, in a specific phase of flight, some of the explanatory variables might demonstrate linear relationship with the fuel flow rate based on physics of aircraft engine operation, separate models need to be fitted in different phases. In that case, simple linear models are excluded from candidate methods. In addition, the collected flight data could be regarded as continuous values; therefore, models for discrete data are excluded.

Aircraft vertical speed measures the ascent and descent rate of aircraft, which may demonstrate fluctuation within a short timespan for many reasons, such as system errors, sensor misreading, and turbulence, shown as Fig. 3. The nature of the vertical speed data indicates that the candidate method has to be robust for outliers. Based on these considerations, the Classification and Regression Trees (CART) is selected for modeling the fuel flow rate.

The CART was introduced by Leo Breiman to refer to a type of Decision Tree algorithms, which can be used for classification or regression predictive modeling problems (Breiman et al., 1984). The visual representation of the CART model is a binary tree, whose leaf node is determined by an if-then statement based on a split point of a variable. Starting from the root node which containing all data points, the CART algorithm recursively split the data with a splitter. The if-then statement is in the form of $X < s$ where s is the splitter and X is a specific explanatory variable. If point satisfies the criteria of $X < s$, it goes to the left side child node, otherwise point goes to the right side child node. The splitting point is selected to minimize the node impurity, which is the heterogeneity of the points within a node. For classification problem,

the Gini index, cross-entropy, and misclassification error are three common criteria of determining the split point. For regression predictive modeling, the least square is used to measure the node impurity. This splitting procedure is to be conducted on explanatory variables until a suitable tree is constructed. The nodes which do not split further are leaf nodes. The value of the leaf node is the predicted value given a set of explanatory variables. A stop criteria is adopted to stop the recursive splitting, which is either when the improvement in mean squared error drops due to further splitting, or when the number of observations in a node reach the predetermined value, or when there is only one observation in the node, or other possible criteria. The recursive partition procedure normally generates very complex trees in terms of nodes and depth which overfits the data. So, a simple tree is preferred as it is easier to interpret. Pruning is widely used to elevate the performance of the tree model. The simplest way of pruning the tree is to work through each leaf node in the tree and evaluate the effect of removing it using out-of-sample data. Leaf nodes are removed if the pruning decreases the mean squared error. Based on the advantages of CART and the features of target data, there are four reasons to use CART in this study case:

1) The nonlinear relationship between the explanatory variables do not affect the model performance;
2) The CART generates a nonparametric model for the variables without knowledge on the complex relationship between the variables;
3) The CART is resistant to the outliers;
4) The tree model is easy to interpret and apply in further study.

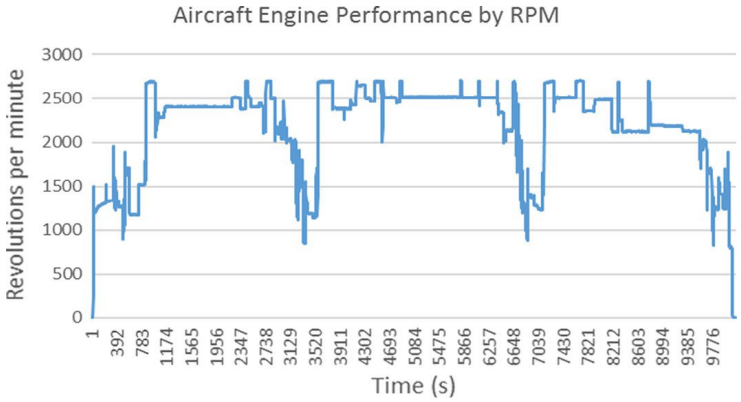

Fig. 1. Aircraft engine performance by revolutions per minute.

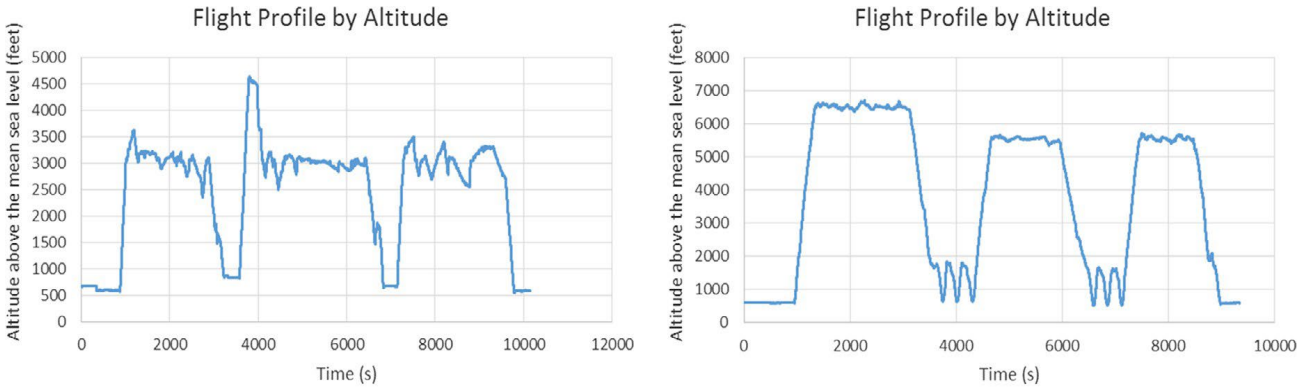

(a)

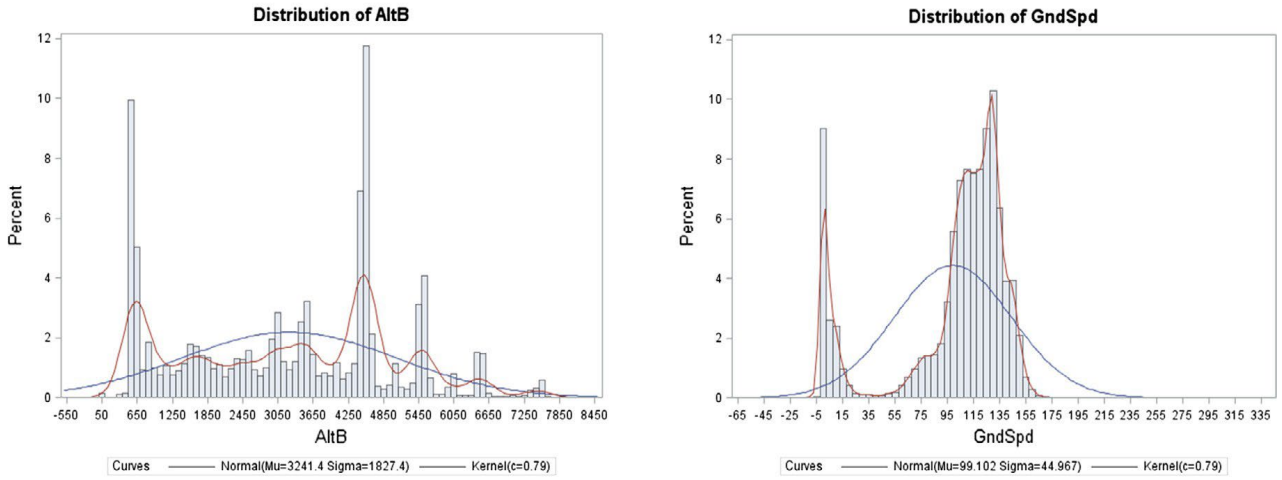

(b)

Fig. 2. (a) Flight profiles by altitude of two flight missions. (b) Distributions of explanatory variables – aircraft barometric altitude and aircraft ground speed in 22 flight missions.

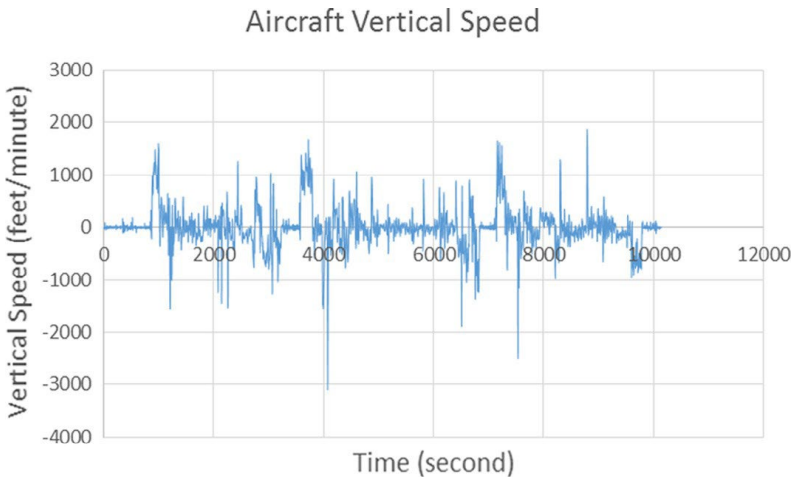

Fig. 3. Aircraft vertical speed.

The CART algorithm helps to predict the fuel flow rate in each phase of flight; however, CART cannot explain the relation- ship between variables. Analyzing the interaction between variables helps understand the rationality of explanatory variable selection. The Smoothing Spline ANOVA (SS-ANOVA) is adopted to further analyze the flight data to understand the selection of variables, the interaction between variables, and the prediction of fuel flow rate.

The SS-ANOVA provides a flexible alternative to the parametric methods for analyzing the relationship of explanatory variables to the response variable, and are now commonly used in many areas such as epidemiology (Gu, 2002). The SS- ANOVA model can capture interactions between variables and the nonlinear relationship between explanatory variables and response variables. On the other hand, the SS-ANOVA model can reduce to a linear model if the data fail to suggest a nonlinear model. The SS-ANOVA models incorporate the ANOVA decomposition for the estimation of a multivariate function as sums of main effect function (of one variable), two-factor interaction functions (of two variables), etc. Especially for regression with Gaussian responses, the problem reduces to be a penalized least squares problem. The general form of penalized least squares functional in a reproducing kernel Hilbert space H = $\bigoplus_{\beta=1}^{p} H_\beta$ can be written as $\frac{1}{n}\sum_{i=1}^{n}(\gamma_i - \eta(x_i)^2 + \psi(\eta)$, where $\mathbf{J}(\mathrm{f}) = \sum_{\beta=1}^{p}\theta_\beta^{-1}$ $(f,f)_\beta$ and $(f, g)_\beta$ are inner products in H_β with reproducing kernels $R_\beta(x,y)$ (Gu, 2002). The smoothing parameters (λ, θ_β) together control the trade-off between fidelity to the data and roughness of the function estimate. The generalized cross-validation (GCV) score is used to select the smoothing parameters (λ, θ_β). Based on the advantages of SS-ANOVA and the features of target data, there are four reasons to use SS-ANOVA in this study case:

1) The SS-ANOVA models can fit the nonlinear relationship.
2) The SS-ANOVA models can capture the interaction between explanatory variables, thus give a good interpretation of the data.
3) The SS-ANOVA models have a rich statistical literature, giving a well-studied model selection procedure.
4) The SS-ANOVA models provide Bayesian Confidence Interval, yielding an assessment of the estimation precision in addition to point estimation.

Modeling

This section presents the modeling setup, and the models constructed from the data using the CART and the SS-ANOVA respectively.

Modeling using the CART

From the data retrieved from the same type of aircraft, 65% of observations are randomly set as the model training partition set and the remaining 35% are the test partition set. Using the CART modeling method, the model of estimating the fuel flow rate is built using the explanatory variables of the aircraft altitude, the ground speed, and the vertical speed. As afore- mentioned, GA aircraft do not always have clear delimitations between phases of flight. In addition, the ICAO engine data- bank does not have complete normalized fuel flow rate for GA reciprocating engines (International Civil Aviation Organization, 2016a,b). In this study, the instantaneous values of explanatory variables are used as input to predict the instantaneous fuel flow rate. The instantaneous fuel flow rate is expected to be valuable on relevant study and applications of GA emissions estimation.

Results of the CART modeling

After partition training with 114,546 observations, a regression tree was generated as shown in Fig. 4. The tree shows that the predicted value depends a series of conditions, which direct the input to different leaf node to be assigned the fuel flow rate. If the input satisfies the condition, it goes to the left side node, otherwise it goes to the right-side node, until the leaf node is reached. For example, when aircraft has ground speed greater than 68.12 knots, vertical speed greater than 352.22 feet per minute but less than 507.60 ft/min, the fuel flow rate at this point is 14.29 gallons per hour. The predictive value of fuel flow rate is believed to be very close to the average fuel flow rate in the particular phase of flight, which will be presented in the section of Output Analysis and Discussion. The tree is not symmetric. The CART fits the data with separate models for each homogenous region of data. This feature improves the accuracy of the model compared to a single regression model.

Also, the model indicates the importance of each explanatory variable/predictor

on predicting the fuel flow rate. As shown in Fig. 5, from the data used in this analysis, the ground speed has the greatest influence on the fuel flow rate, the vertical speed has the median influence on the fuel flow rate, and the aircraft altitude has little influence on fuel flow rate, which is roughly accordant to the characteristics of actual GA operations.

The mean absolute error (MAE), shown as Eq. (2), is used to measure the average magnitude of the errors in the set of the predicted values. The final developed model has an MAE of 1.244, the lowest of the candidate models.

$$\text{MAE} = \frac{SAE}{N} = \frac{\sum_{i=1}^{N}|x_i - \hat{x}_i|}{N} \qquad (2)$$

where x_i is the observations time series, $\hat{x}_i$ is the predicted time series, N is the number of data points, *SAE* is the sum of the absolute errors (or deviations).

Modeling using the SS-ANOVA

The Smoothing Spline ANOVA is used to model the fuel flow rate to explore the relationship between selected explanatory variables using the same datasets as the CART algorithm. A new sample of 65% of total observations (104,863 observations) are randomly selected as the model training partition set and the remaining 35% are the test partition set. The aircraft altitude, the ground speed, and the vertical speed are the explanatory variables in the SS-ANOVA as in the CART.

The fuel flow rate is modeled as (*VSpd, GndSpd, AltB*) + ε where f is a function of *VSpd* – the aircraft vertical speed, *GndSpd* – the aircraft ground speed, and *AltB* – the aircraft altitude by barometric altimeter, and the noise ε~N(0, σ^2). Basically, f(*VSpd, GndSpd, AltB*) could be illustrated as $\beta_0 + \beta_V VSpd + \beta_G GndSpd + \beta_A AltB$, where β_0 β_V β_G β_A are the coefficients, which is actually a linear model. In our case, an ANOVA decomposition can be defined as $f = (I - A_\gamma + A_\gamma)f$, where I is the identity operator, A_γ s are averaging operators acting respectively on arguments *VSpd*; *GndSpd and AltB*. An example of A_γ could be A1 = f(0, GndSpd, AltB), A2 = f(VSpd, GndSpd, 0). Thus , one has f = $f + f_v + f_G + f_A + f_{v,G} + f_{v,A} + f_{G,A} + f_{v,G,A}$, where

$f = f(0, 0, 0)$,

$f_v = f(VSpd, 0, 0) - f(0,0,0)$, $f_G = f(0, GndSpd, 0) - f(0,0,0)$ $f_A = f(0,0,AltB) - f(0,0,0)$,

$f_{v,G} = f(VSpd, GndSpd, 0) + f(0,0,0) - f(VSpd, 0,0) - f(0, GndSpd, 0)$,

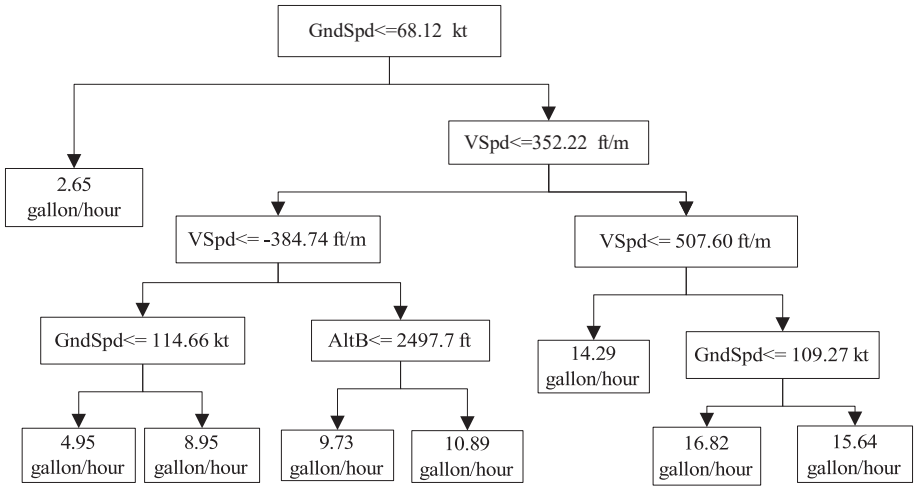

Fig. 4. The CART regression tree for predicting the fuel flow rate of Cirrus SR-20 aircraft. Note, *GndSpd*: aircraft ground speed, *VSpd*: aircraft vertical speed, *AltB*: aircraft altitude by barometric altimeter.

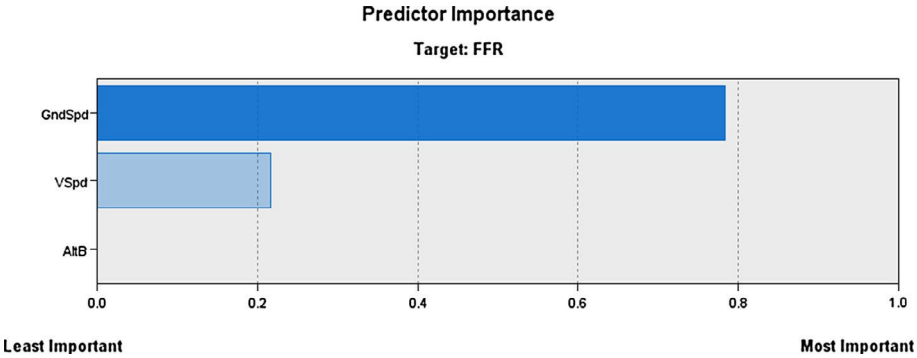

Fig. 5. Predictor importance on predicting the fuel flow rate.

$$f_{v,A} = f(VSpd,0,AltB) + f(0,0,0) - f(VSpd,0,0) - f(0,0,AltB),$$

$$f_{G,A} = f(0, GndSpd, AltB) = f(0,0,0) - f(0, GndSpd,0) - f(0,0,AltB),$$

$$f_{v,G,A} = f(VSpd, GndSpd, AltB) - f(0,0,0) + f(VSpd,0,0) + f(0,GndSpd,0) + f(0,0,AltB) - f(VSpd, GndSpd, 0) - f(VSpd,0,AltB) - f(0,GndSpd, AltB).$$

Note that it is straightforward to obtain similar results with different averaging operators.

Modeling selection

ANOVA structures provide a better understanding of the model; however, it brings about a new question: can redundant terms be eliminated by a selection procedure? The classical testing like a *t* test relies on the determined sampling distribution. However, due to the infinite dimension of the nulls space, it is hard to

determine the sampling distribution for SS- ANOVA. Thus, it is difficult to adapt the classical testing to the modeling situation in this study. However, an approach based on the Kullback-Leibler geometry was developed in Gu is expected to be applicable in this case (Gu, 2002). For example, H_0 : f ϵ $\mathcal{H}_0 \oplus \mathcal{H}_1$, where $\mathcal{H}_0$ = {f : f = $f + f_v + f_G + fA + f_{V,G} + f_{V,A} + f_{G,A}$} and $\mathcal{H}_1$ = {f : F = FV,G,A}. One calculates an estimate $\hat{f} \epsilon \mathcal{H}_0 \oplus \mathcal{H}_1$, obtains its Kullback-Leibler projection $\tilde{f} \epsilon \mathcal{H}_0$ by minimizing a setting-specific KL($\hat{f}$, f) over f ϵ $\mathcal{H}_0$ then an ‘‘entropy decomposition”, KL($\hat{f}$,f_c) = KL($\hat{f}$, $\tilde{f}$) + KL($\tilde{f}$, f_c), can be inspected, where f_c is a degenerate fit, such as a constant regression function or a uniform density. When the ratio of KL($\hat{f}$, $\tilde{f}$)/KL($\tilde{f}$, f_c) is small, one loses little by cutting out $\mathcal{H}_1$. Note that cutting out H_1 is equivalent to elimination of the interaction $f_{V,G,A}$.

Results of the SS-ANOVA modeling

The basic data analysis indicates that the distribution of the dependent variable – the Fuel Flow Rate (*FFlow*) is very skewed, therefore, the *FFlow* is transformed as $\log_{10}$ð*FFlow* þ 1Þ. After model selection, the final model is shown as Eq. (3), and the MAE = 1.086.

$$\widehat{\mathrm{FFlow}} = C + f_V(VSpd) + f_G(GndSpd) + f_{VG}(VSpd, GndSpd) \qquad (3)$$

where C is a constant, *FFlow* is the fuel flow rate, *VSpd* is the aircraft vertical speed, *GndSpd* is the aircraft ground speed, $f_{V(.)}$ represents the main effect of *VSpd* on *FFlow*, $f_{G(.)}$ represents the main effect of *GndSpd* on *FFlow*, and $f_{V,G(.)}$ represents the interaction effect of *VSpd* and *GndSpd*.

The main effect of aircraft vertical speed on the fuel flow rate is shown as Fig. 6. The effect increases as aircraft vertical speed increases. The aircraft vertical speed demonstrates the largest contribution to the fuel flow rate when aircraft is rapidly ascending, which could be the phase of takeoff or during the ascending in the phase of cruise, and has the smallest contribution to the fuel flow rate during the phase of landing or descending in cruise. It is notable that the main effect could be negative in this case, because the *FFlow* is transformed as $\log_{10}$(*FFlow* +1), and there is a constant C in the model log10($\widehat{\mathrm{FFlow}}$ +1) = C +f_V(VSpd) + f_G(GndSpd) + f_{VG} (VSpd, GndSpd) to make sure that $\widehat{\mathrm{FFlow}}$ is always positive. Essentially, the negative effect of vertical speed in

this model only indicates less contribution of vertical speed to the fuel flow rate compared to the positive effect of vertical speed.

The main effect of aircraft ground speed on the fuel flow rate is shown as Fig. 7. The main effect increases as aircraft ground speed increases. The graph shows that the curve is almost linear with a narrow confidence band from 20 knots of *GndSpd* to 140 knots of *GndSpd*. But when the ground speed is below 20 knots or above 140 knots, the confidence band becomes wider, and the main effect of *GndSpd* $f_G(.)$ is almost a horizontal line. The lack of data at the two edges results in a large standard deviation. There are two possible explanations: The first possibility could be the lack of data at the two edges results in large standard deviation. The second possibility might be explained from the aircraft operations. Actually, when the ground speed is below 20 knots, the aircraft was most likely taxiing on the ground, that is to say aircraft was moving with or without temporary stops, like holding still at somewhere on the runway or taxiway. During that phase, the performance of aircraft engine is extremely irregular, therefore, the confidence band is relatively wider than the medium part of this curve. On the other hand, when aircraft ground speed is above 140 knots, the effect could be determined by the actual operational environment. For example, if the aircraft of Cirrus SR-20 in this study was flying with 0 head wind, when the aircraft ground speed was above 140 knots, aircraft airspeed was getting close to the maximum cruise airspeed of 155 KTAS (Cirrus Design, 2011). Assuming pilots kept aircraft true airspeed below the maximum cruise airspeed, the aircraft was more likely flying with tail wind when the ground speed was getting much higher than 140 knots. In that case, the tail wind might help explain the reduce of the effect of the ground speed.

The interaction effect of aircraft vertical speed and aircraft ground speed is described as Fig. 8; Fig. 9 shows the standard deviation of the interaction effect. Three cases of the interaction effect are illustrated here.

First, the color of blue[3] represents that the interaction has a strong and negative effect on $\log_{10}(FFlow+1)$. The up-right corner of Fig. 8 describes the flight status with

[3] For interpretation of color in 'Figs. 8 and 9', the reader is referred to the web version of this article.

extremely large positive vertical speed and high ground speed. Dark blue in this area indicates that the coherent contribution of aircraft vertical speed and ground speed does not contribute to the fuel flow rate. Theoretically, the aircraft type analyzed in this study is not able climb with that vertical speed while flying over 150 knots in ground speed. The occurrence of this area is very likely to be noisy data or caused by upwash or air turbulence since violent air turbulence could rapidly increase vertical speed and ground speed. The negative influence in this area compensates the large positive main effect on $\log_{10}(FFlow + 1)$ from vertical speed and ground speed. This could be explained by the situation that an aircraft engine throttles back to descend and maintain the flight level. The left side blue area describes the flight status with negative vertical speed and slow ground speed, which is very likely during the phase of approach or landing. Second, the green area describes the case when the interaction effect is around 0, which means the sum of two main effects could well model the fuel flow rate, the interaction effect of vertical speed and ground speed does not contribute to the fuel flow rate. Third, the lower right-side yellow triangular area very likely describes the opposite situation of the upper right-side blue area. The aircraft was possibly experiencing downwash or air turbulence, which could rapidly cause a loss of altitude. To maintain the flight level, the aircraft engine is throttled up and has an increased fuel flow rate. For the upper-left corner area in yellow reasonably describes the phase of takeoff with positive vertical speed and small ground speed. The interaction effect of these two variables positively contribute the fuel flow rate.

Output analysis and discussion

Two modeling techniques were explored to develop a model of fuel flow rate of GA piston engine aircraft. First, the model developed using the CART was interpreted from the standpoint of phases of flight of GA Landing and Takeoff (LTO) cycle (Huang and Johnson, 2016; Katsaduros et al., 2014). Because the working mode of piston engines in the takeoff phase has no significant difference from that in the phase of climb-out, the phases of takeoff and climb-out are merged. In that case, the original four phases of flight of the LTO cycle for turbine engine aircraft is simplified into three phases of flight: Taxi/Idle, Takeoff, and Approach (Huang and Johnson, 2016; Swiss

Federal Office of Civil Aviation, 2007).

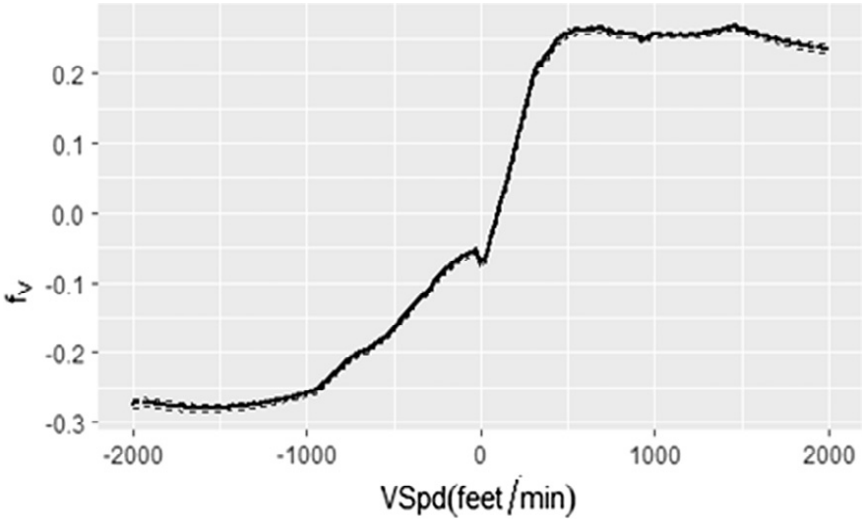

Fig. 6. Main effect of *VSpd* with 90% confidence interval.

Aircraft targeted in this study are based at the Purdue University Airport. In the data, the elevations of airports involved in these flight missions are around 625 ft. The LTO only considers operations under 3000 ft above the ground level (AGL). Based on above conditions and the aircraft attitude in each phase of flight, for example, aircraft has negative vertical speed when descending, and the aircraft altitude should be less than 3000 ft AGL. The leaf nodes of the regression tree are classified into each phase of flight. Shown as Table 1. The leaf nodes of 10.89 gallons per hour and 14.29 gallons per hour are assumed to be more fit the out of LTO operations in regards to the corresponding partition conditions. Generally, the CART model provides a very straightforward outcome of the fuel flow rate for each phase of flight in the LTO cycle.

To further examine the performance of the CART model, descriptive statistical analysis was conducted on the original dataset. The *t*-test was used to compare the average fuel flow rate in each phase of flight manually calculated from the original dataset with the outputs of the CART model. We assume in the null hypothesis that the mean of the model outputs of the FFR is not significantly different from the mean of the FFR manually calculated from the original data for a particular phase of flight. If the p-value for the *t*-test is less than a critical a = 0.05, then the average fuel flow rate in a particular phase of flight determined by the CART model is significantly different from

the mean of fuel flow rate defined by the general aviation LTO cycle, thus we reject the null hypothesis (H_0).

The original flight data were classified into the same three phases of flight of the LTO cycle based on the phases of flight of the GA LTO cycle (Huang and Johnson, 2016; Katsaduros et al., 2014). The results of *t*-test are shown as Fig. 10 and Table 2.

The one-sample *t*-test indicates that the average fuel flow rate of the phase of taxi and takeoff predicted by the regression model is not significantly different from the average fuel flow rate derived from the original flight data. However, the predicted average fuel flow rate of the phase of approach is significantly different from the corresponding value derived from the original flight data. Possible explanations for the difference could originate from the flight data source, the method of deriving the average value of the original flight data, or the inaccuracy of the regression tree. Because the flight data come from training flights, it is understandable that student pilots may not be generally capable of smoothly adjusting the aircraft status for approaching and landing. In that case, the fuel flow rate would be very hard to predict by the regression model. Further study is need to exclude other possible influence on predicting the fuel flow rate in the phase of approach. Still, the developed regression model demonstrates a good performance on predicting the fuel flow rate of the phases of takeoff and taxi/idle in the LTO cycle.

Shown as Fig. 5, explanatory variables demonstrate different influence on fuel flow rate. Aircraft ground speed has the greatest influence on fuel flow rate, vertical speed has less influence, and aircraft altitude has little influence on fuel flow rate. The SS-ANOVA helps to explore the relationship between variables. The model developed using the SS-ANOVA eliminates the explanatory variable of the aircraft altitude, because the model developed using the SS-ANOVA is in accordance with the result of the CART model that the aircraft altitude has little contribution to the response variable of fuel flow rate. Possible explanation for that phenomenon could be that: Unlike the turbine engine aircraft operating in a large range of altitude, piston-engine aircraft are more likely flying below 10,000 ft. The flight altitudes in this study are primarily between 3500 ft and 5500 ft. In that case, the difference of atmospheric density in that range of flight altitude is not as large as that faced by turbine engine aircraft; therefore, aircraft

altitude might not cause significant influence on the fuel flow rate of air- craft piston engine.

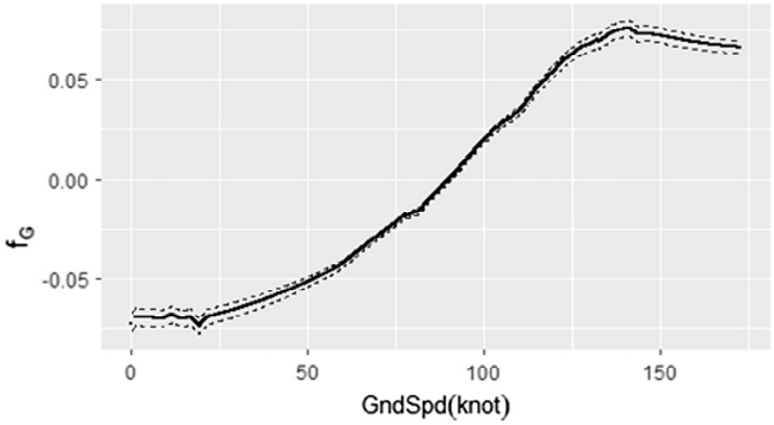

Fig. 7. Main effect of *GndSpd* with 90% confidence interval.

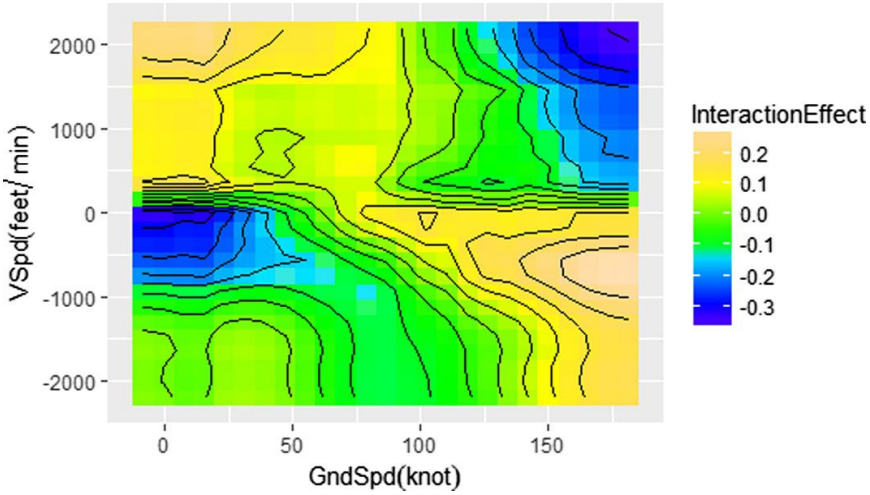

Fig. 8. Interaction effect of *VSpd* and *GndSpd.*

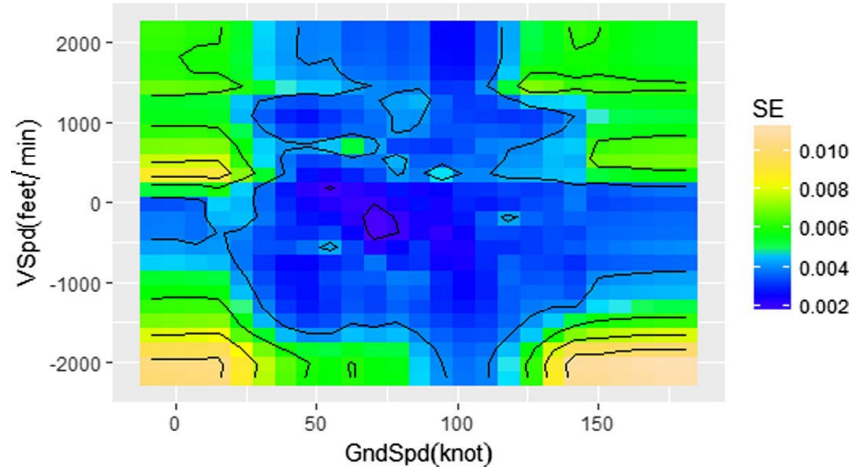

Fig. 9. Standard deviation interaction effect of *VSpd* and *GndSpd.*

Table 1: Leaf node classification by phases of flight.

Phase of flight	Leaf nodes	Average FFR
Taxi/idle	2.65 gallon/hour	2.65 gallon/h
Takeoff	16.82 gallon/hour; 15.64 gallon/hour	16.23 gallon/h
Approach	4.95 gallon/hour; 8.95 gallon/hour; 9.73 gallon/hour	7.88 gallon/h
Out of the LTO	10.89 gallon/hour; 14.29 gallon/hour	NA

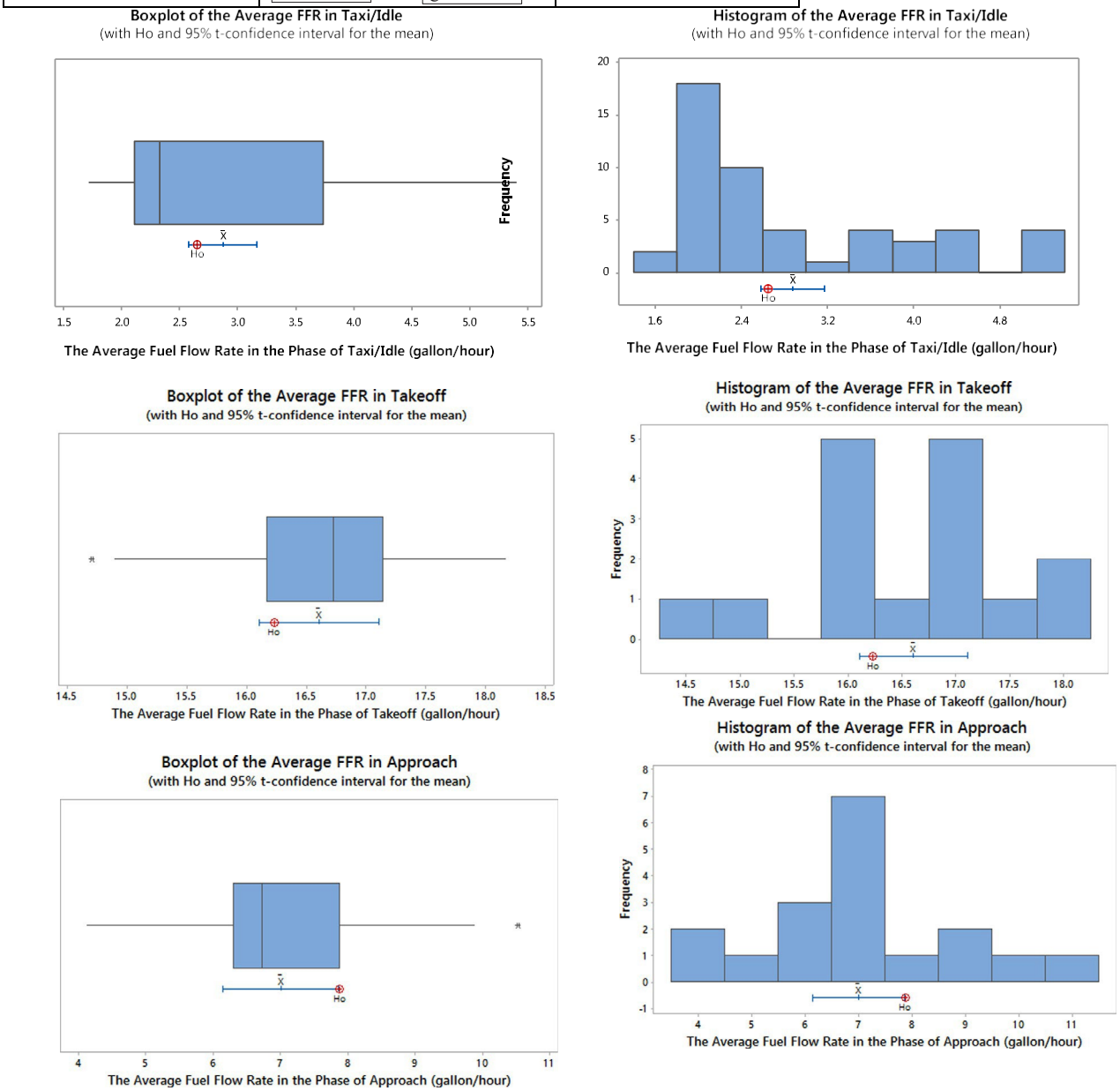

Fig. 10. The graphical description of one-sample *t*-test results of the fuel flow rate of each phase of flight.

Table 2: The *t*-test result of the fuel flow rate by phases of flight.

Phase of flight	Predicted FFR (gallon/h)	FFR from original data (gallon/h)	P-value (for *t*-test $\mu_1 = \mu_2$ *vs* $\mu_1 \neq \mu_2$)
Taxi/idle	2.65	2.87	0.138*
Takeoff	16.23	16.61	0.130*
Approach	7.88	7.01	0.047*

*Significant at **α** = 0.05.

In addition to the description of the interaction between explanatory variables, the developed model using the SS-ANOVA can also predict the instantaneous fuel flow rate based on aircraft ground speed and vertical speed with the MAE = 1.086 smaller than 1.244 of the MAE of the CART model, indicating the SS-ANOVA model has better accuracy than the CART model. Although SS-ANOVA has the assets of better describing the interaction between variables, and being more flexible for the distribution of data and the relationship between variables, the SS-ANOVA is not as robust to outliers as the CART model. On the contrary, the CART model well fit the characteristics of irregular flight data due to the flexible operations of general aviation. Also, the output of the CART model is more intuitive to interpreted by the phases of flight, so that is more easy to be applied in quick prediction of the fuel flow rate.

Conclusion

This study explores two nonparametric models to predict the fuel flow rate of GA piston-engine aircraft in each phase of flight of the LTO cycle. By applying the machine learning technique, the CART model is believed to be robust for flight data outliers caused by the flexible GA operations, random system errors, and other unknown factors. The operational flight data from Purdue University Cirrus SR-20 fleet was used in training and testing the CART model. The CART model intuitively describes the fuel flow rate by phases of flight, and demonstrates straightforward logic of predicting the fuel flow rate. That feature is expected to help simplify the procedure of predicting the fuel flow rate quickly and accurately. In addition, the Smoothing Spline ANOVA was adopted to remodeling the fuel flow rate and further explore the relationship between variables. Both models demonstrate good accuracy in predicting the fuel flow rate and reflect that aircraft altitude has less influence on the fuel flow rate of piston engine

aircraft used in this study. The analysis results are believed to be reasonable from the perspective of actual flight operations.

However, for the phase of approach, it is noticeable that the predicted fuel flow rate by the CART model is significantly different from the derived value based on the GA LTO cycle. Possible reasons could be: (1) flight data comes from flight training aircraft which were operated by pilot students; inexperience operations in approach phase might generate large amount of noisy data; (2) the method of deriving the average fuel flow rate from the original flight data could generate errors; (3) inaccuracy of the CART model. In the meantime, the SS-ANOVA model is not easy to be interpreted by the phases of flight while giving more information about the interaction between variables. These two models are still subject to further evaluation and validation before being applied in industry, and are expected to provide references for further study on practical approaches of exhaust emissions estimation of general aviation.

References

Automatic Dependent Surveillance-Broadcast (ADS-B) Out Equipment and Use. Part 91, 41 C.F.R. § 91.225.

Automatic Dependent Surveillance-Broadcast (ADS-B) Out Equipment Performance Requirements. Part 91, 41 C.F.R. § 91.227.

Baklacioglu, T., 2016a. Fuel flow rate modelling of transport aircraft for the climb flight using genetic algorithms. Aeronaut. J. 119 (1212), 173–183.

Baklacioglu, T., 2016b. Modeling the fuel flow rate of transport aircraft during flight phases using genetic algorithm-optimized neural networks. Aerosp. Sci. Technol. 49 (2016), 52–62.

Breiman, L., Friedman, J., Stone, C.J., Olshen, R.A., 1984. Classification and Regression Trees. CRC Press.

Chati, Y.S., Balakrishnan, H., 2016. Statistical modeling of aircraft engine fuel flow rate. In: 30th Congress of the International Council of the Aeronautical Science, DCC, Daejeon, Korea; September 25–30, 2016.

Cirrus Design, 2011. Airplane Information Manual for the Cirrus Design SR20.

Available at: <http://www.cospilot.com/files/SR20_POH.pdf> (accessed 7 Jan 2017).

Collins, B.P., 1982. Estimation of aircraft fuel consumption. J. Aircraft 19 (11), 969–975.

EUROCONTROL, 2016. Modelling Tools to Measure the Environmental Impacts of Aviation. Available at: <http://www.eurocontrol.int/environment- modelling-tools> (accessed 18 July 2016).

European Union, 2008. Directive 2008/101/EC of the European Parliament and of the Council. Available at: < http://eur-lex.europa.eu/legal-content/EN/TXT/ PDF/?uri=CELEX:32008L0101&from=EN > (accessed 15 July 2016).

General Aviation Manufacturers Association, 2016. 2015 General Aviation Statistical Databook & 2016 Industry Outlook. Available at: <https://www.gama. aero/files/GAMA_2015_Databook_LoRes%20updated%203-29-2016.pdf> (accessed 13 Jan 2017).

Gu, C., 2002. Smoothing Spline ANOVA Models. Springer-Verlag, New York.

Huang, C., Johnson, E.M., 2016. Fuel flow rate and duration of general aviation landing and takeoff cycle. In: 16th AIAA Aviation Technology, Integration, and Operations Conference, Washington, DC, 2016.

International Air Transport Association, 2013. IATA Annual Review 2013. Available at: <https://www.iata.org/about/Documents/iata-annual-review-2013- en.pdf> (accessed 15 July 2016).

International Air Transport Association, 2016. A Global Approach to Reducing Aviation Emissions. First Stop: Carbon Neutral Growth from 2020. Available at: <http://www.iata.org/whatwedo/environment/Documents/global-approach-reducing-emissions.pdf> (accessed 20 July 2016).

International Civil Aviation Organization, 2008. Environmental Protection (Annex 16, Volume II), third ed., 2008. Available at: <https://law.resource.org/ pub/us/cfr/ibr/004/icao.annex.16.v2.2008.pdf> (accessed 15 July 2016).

International Civil Aviation Organization, 2011. Airport Air Quality Manual (Doc 9889), first ed., 2011. Available at: <http://www.icao.int/publications/

Documents/9889_cons_en.pdf> (accessed 15 July 2016).
International Civil Aviation Organization, 2016. CAEP Description, Environmental Protection. Available at: <http://www.icao.int/environmental-protection/Documents/CAEP/Images/CAEPDescription.jpg> (accessed 15 July 2016).
International Civil Aviation Organization, 2016. Emissions Databank (Version 23 of 11/2016). ICAO Aircraft Engine Emissions Databank. Available at: <https://www.easa.europa.eu/node/15672> (accessed 18 January 2017).
Katsaduros, D., Prall, M., Johnson, M.E., 2014. Exploration of emissions modeling for a general aviation airport. In: 52nd Aerospace Science Meeting, AIAA SciTech Forum, National Harbor, Maryland, 2014..
Khadilkar, H., Balakrishnan, H., 2012. Estimation of aircraft taxi fuel burn using flight data recorder archives. Transport. Res. Part D: Transp. Environ. 17 (7), 532–537.
Swiss Federal Office of Civil Aviation, 2007. Summary Report of Aircraft Piston Engine Emissions. Federal Office of Civil Aviation, Aviation Policy and Strategy, Environmental Affairs, June 2007.
U.S. Environmental Protection Agency, 1985. Compilation of Air Pollutant Emission Factors Volume II, Mobile Sources (AP-42). US Environmental Protection Agency, Ann Arbor, Michigan, September 1985.
U.S. Federal Aviation Administration, 2005. Aviation & Emissions A Primer. Federal Aviation Administration, Office of Environment and Energy, Washington, DC, January 2005.
U.S. Federal Aviation Administration, 2014. General Aviation and Part 135 Activity Survey-CY 2014, Chapter II. Common General Aviation and Taxi Measures. FAA Aviation Data & Statistics. Available at: <http://www.faa.gov/data_research/aviation_data_statistics/general_aviation/CY2014/> (accessed 15 July 2016).
U.S. Federal Aviation Administration, 2017. Aviation Environment Design Tool. Available at: <https://aedt.faa.gov/2c_information.aspx> (accessed 16 Jan 2017).